Contents of Today

Review previous

Spinodal Points

Compounds

etc.

Applications of phase diagrams

Conclusion Remarks

Examples

Review of Today

- Immiscibility
- Spinodal Points
- Compounds
- Summary of Binary Phase
- Ternary Phases Reaction in Binary Systems
- 二元相图构成的规则

Binary System

Degrees of freedom available in the system (F):

$$F = C - P + 1$$

$$F = C - P + 2$$

F: the number of system variables that we may freely vary, or arbitrarily fix
C: components
P: phase

$$C = 2$$

$$P = 1, F = 2$$ 单相区

$$P = 2, F = 1$$ 平衡线包围的两相区

$$P = 3, F = 0$$ 三相平衡线

单元系

- F=C-P+2=3-P
- 两相共存F=1
  - 给定温度或压力，体系就已确定，因为两相均为纯物质

二元系

- F=C-P+1=3-P
- 两相共存F=1
  - 给定温度或压力，体系如果要确定，必须给定两相中的组成，即浓度
  - 多相平衡条件给出，

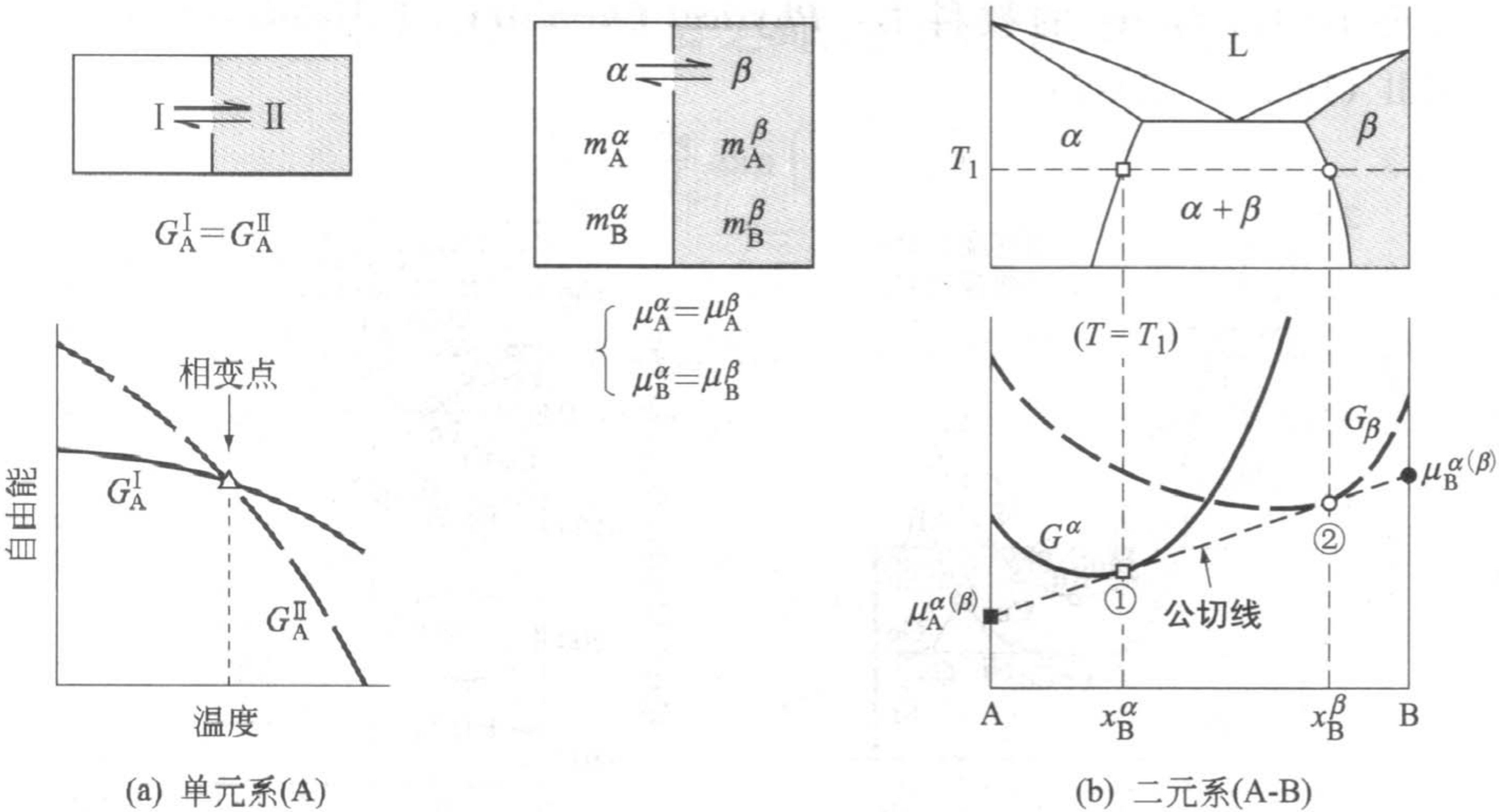

图 4.1　单元系和二元系的两相平衡条件

（a）单元系中自由能的交叉点是平衡温度；（b）二元系中公切线的切点①和②是平衡成分

T. Nishizawa

固液完全互溶的体系

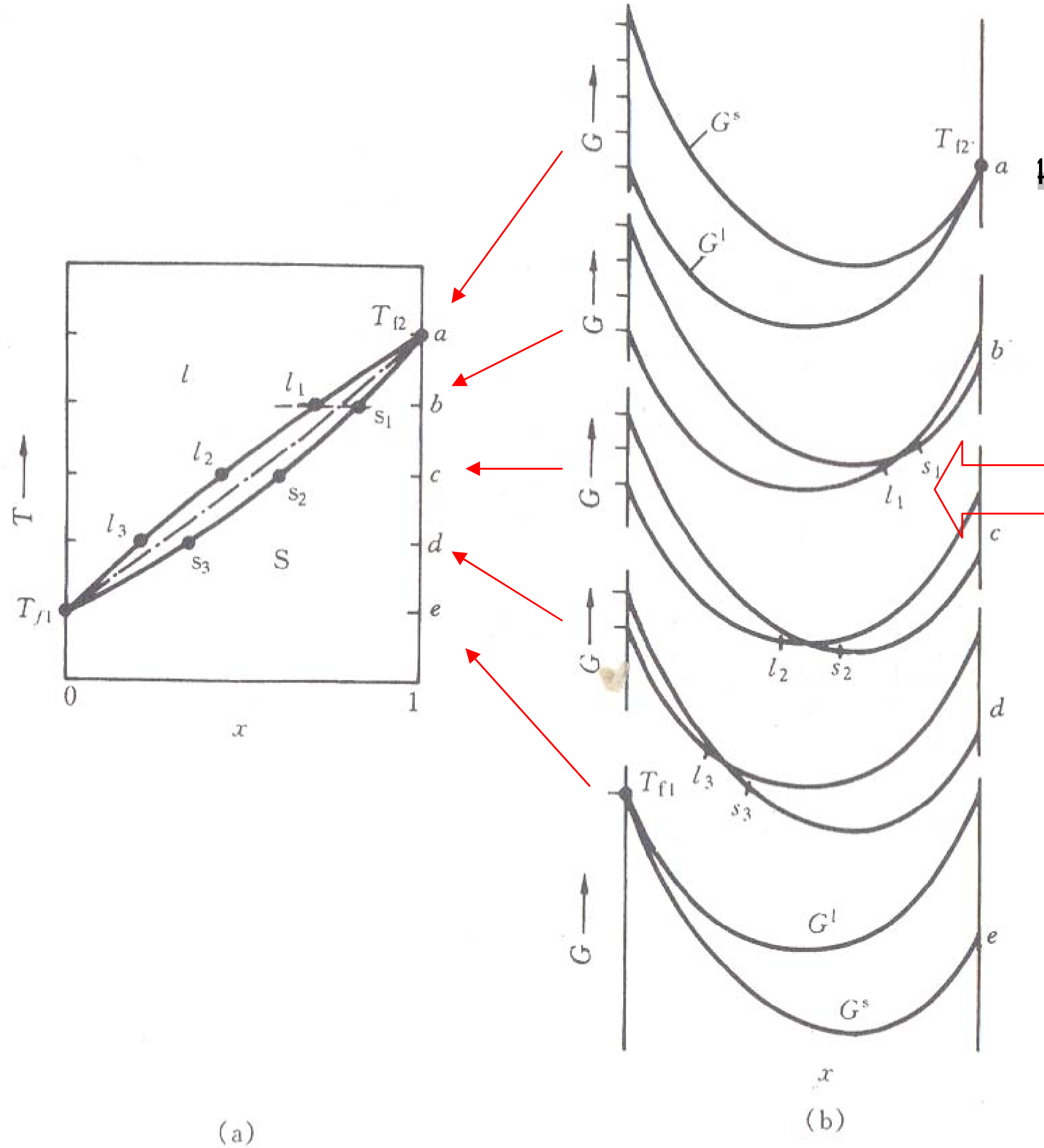

图 6-9　两组元完全互溶的相图

Sn-Bi

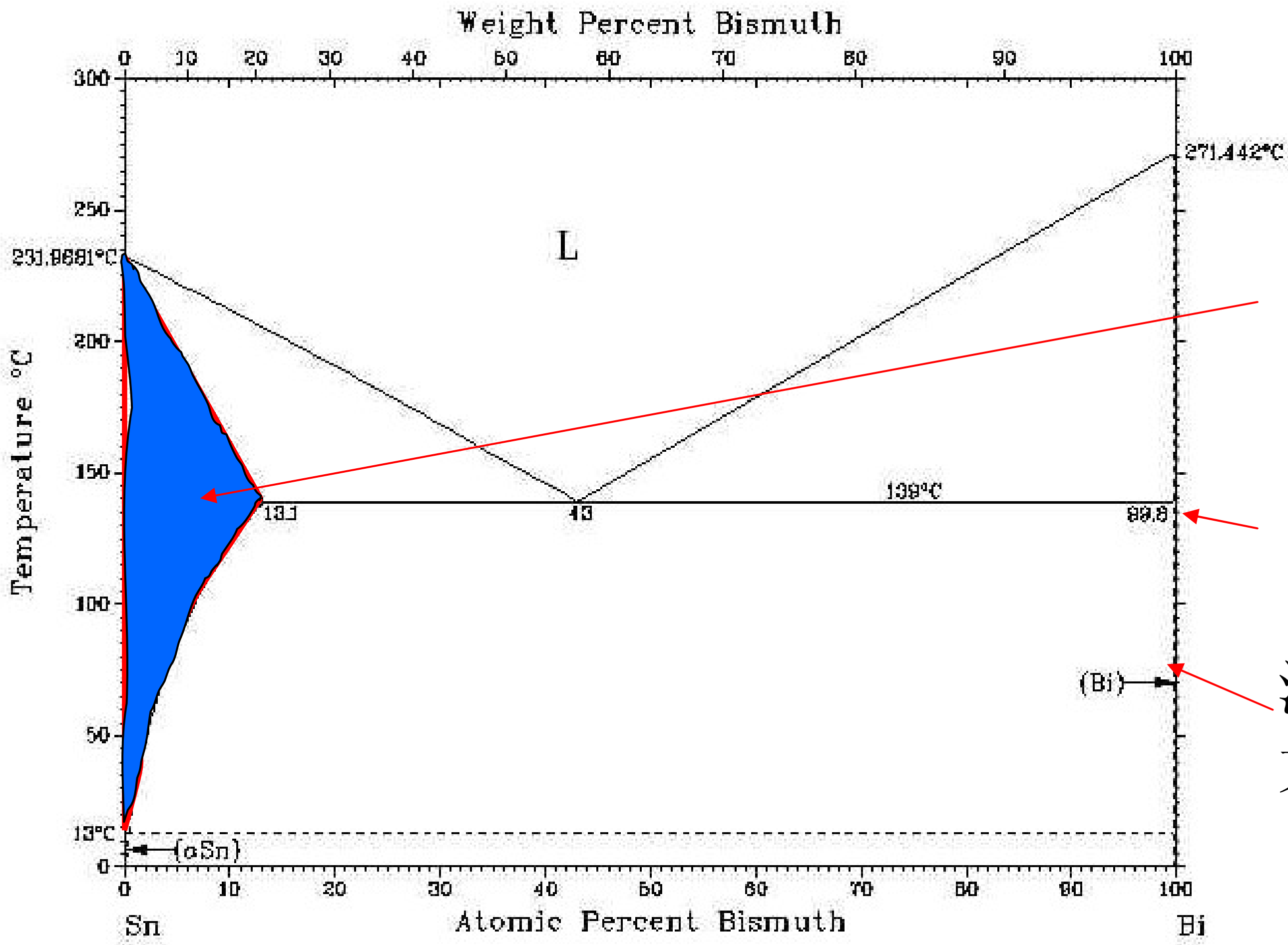

Sn中溶有Bi形成固溶体

自由度2

溶解度变化很大！

Spinodal Points

Spinodal points

A special significance in the study of phase transformations

$$\left(\frac{\partial^2 G_M}{\partial x_B^2}\right)_T = RT\left(\frac{1}{x_A}+\frac{1}{x_B}\right) - 2\varpi = 0$$

$$x_A x_B = \frac{RT}{2\varpi}$$

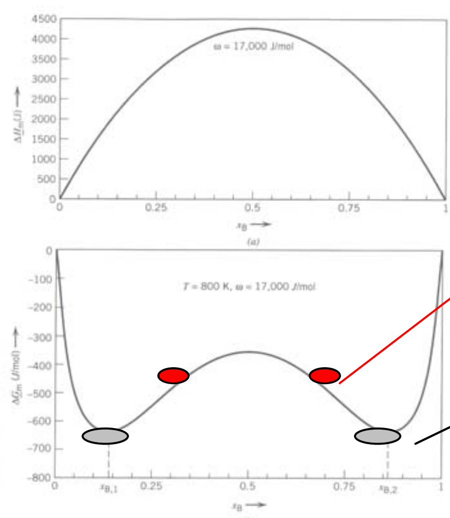

Figure 9.13 Plots of properties of mixing versus composition for regular solutions: (a) molar enthalpy and (b) molar Gibbs free energy.

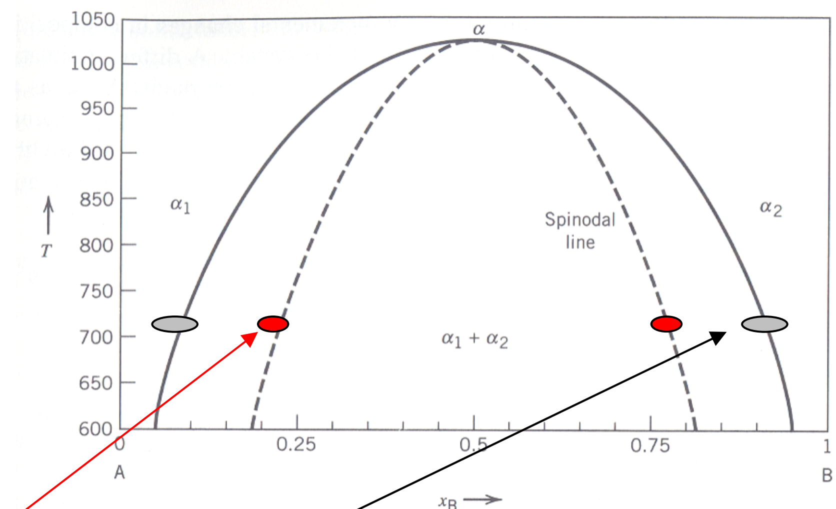

Figure 9.15 The miscibility gap, showing spinodal line.

Gibbs free energy of mixing curve is concave downward
In this region the solution may begin the process of decomposition into the equilibrium phases by incremental changes in composition without increasing the total Gibbs free energy of the system.

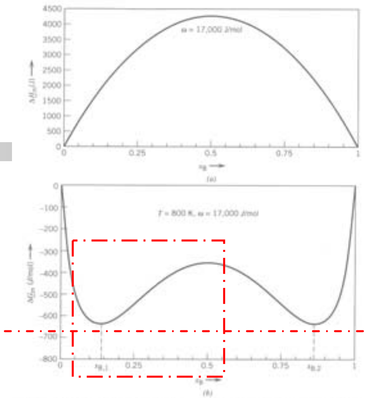

Figure 9.13 Plots of properties of mixing versus composition for regular solutions: (a) molar enthalpy and (b) molar Gibbs free energy.

To the left of the spinodal point
The transformation is discontinuous

To the right of the spinodal point
The transformation is continuous

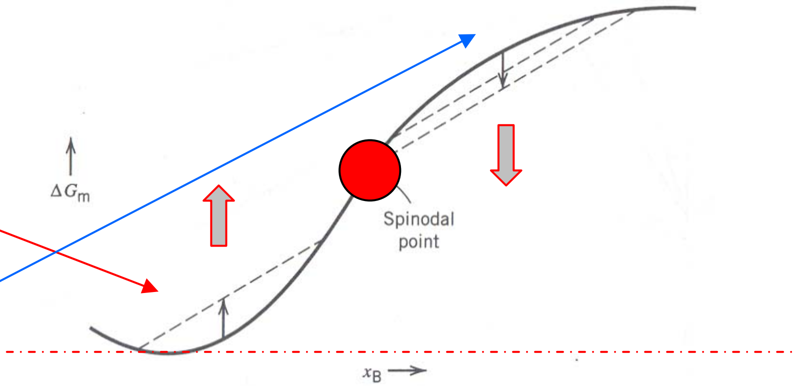

Figure 9.16 The relation between Gibbs free energy of mixing and composition on either side of spinodal point.

X_B

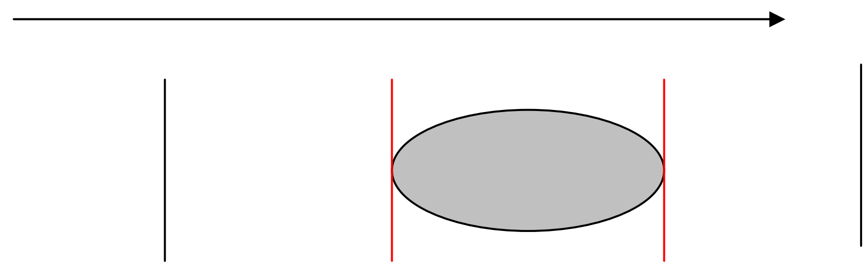

存在溶解度间隙的相图

非理想

规则溶液

相律

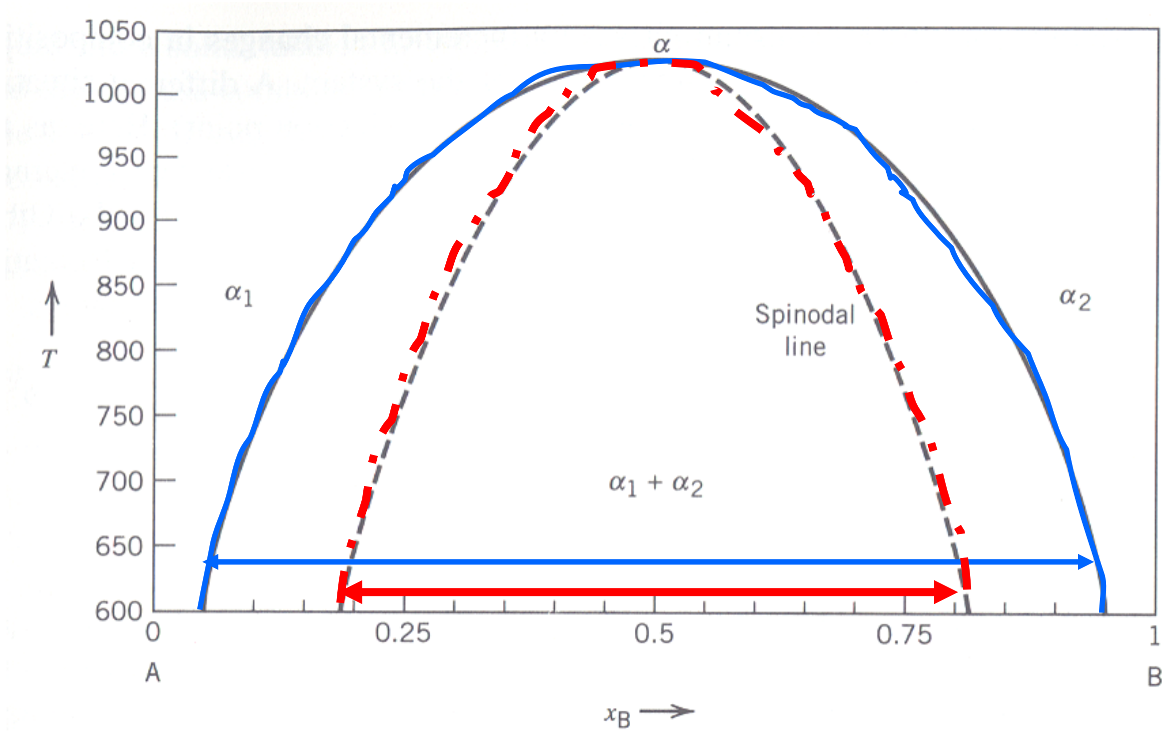

Figure 9.15 The miscibility gap, showing spinodal line.

两相区的组成和数量解析

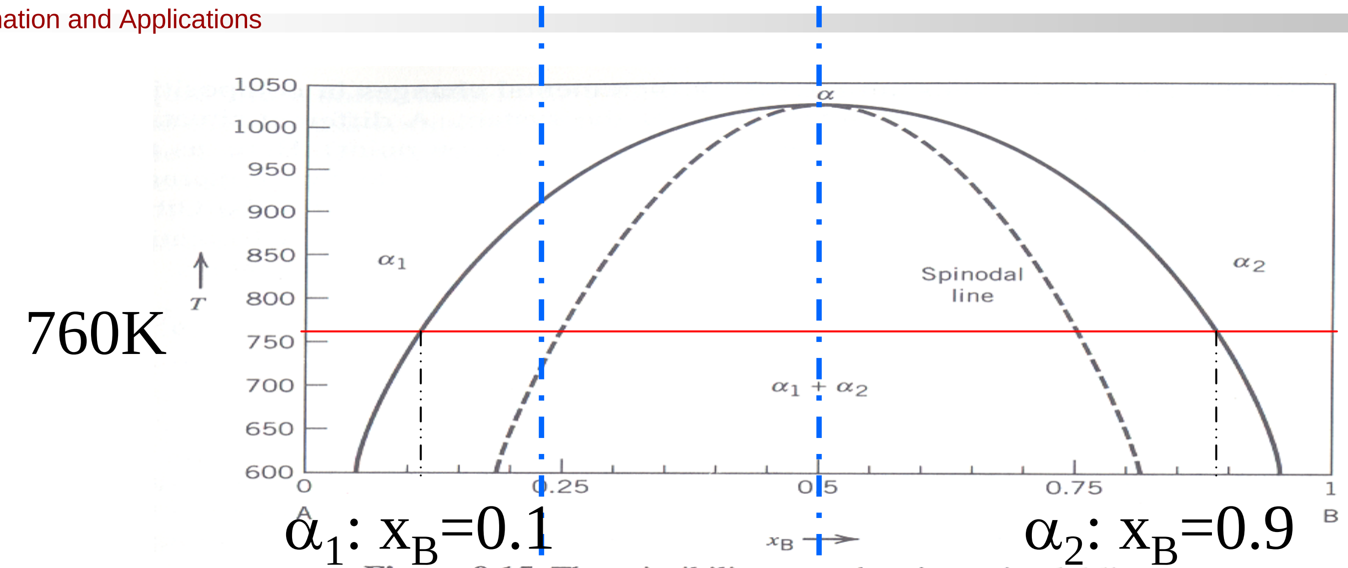

Figure 9.15 The miscibility gap, showing spinodal line.

I: x_B=0.2　　　II: x_B=0.5

体系	I：x_B＝0.2		II：x_B＝0.5	
平衡组成	α_1	α_2	α_1	α_2
	x_B＝0.1	x_B＝0.9	x_B＝0.1	x_B＝0.9
平衡相的量	7/8	1/8	4/8	4/8

Peritectic Phase Diagrams

Peritectic transformation
A liquid phase and a solid phase can combine to form an entirely new solid phase

$$liquid + solid_{\alpha} = solid_{\beta}$$

$$liquid + solid_{\delta} = solid_{\gamma}$$

相律？

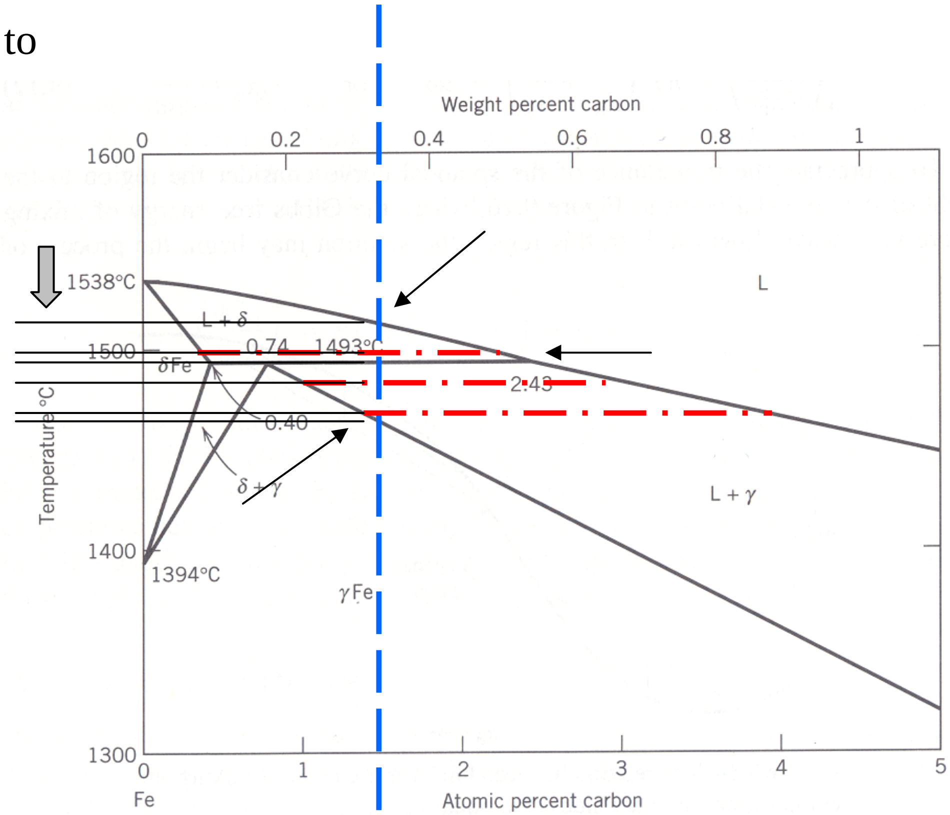

Figure 9.17 The binary phase diagram for carbon (graphite) and iron.

Mg-Pb

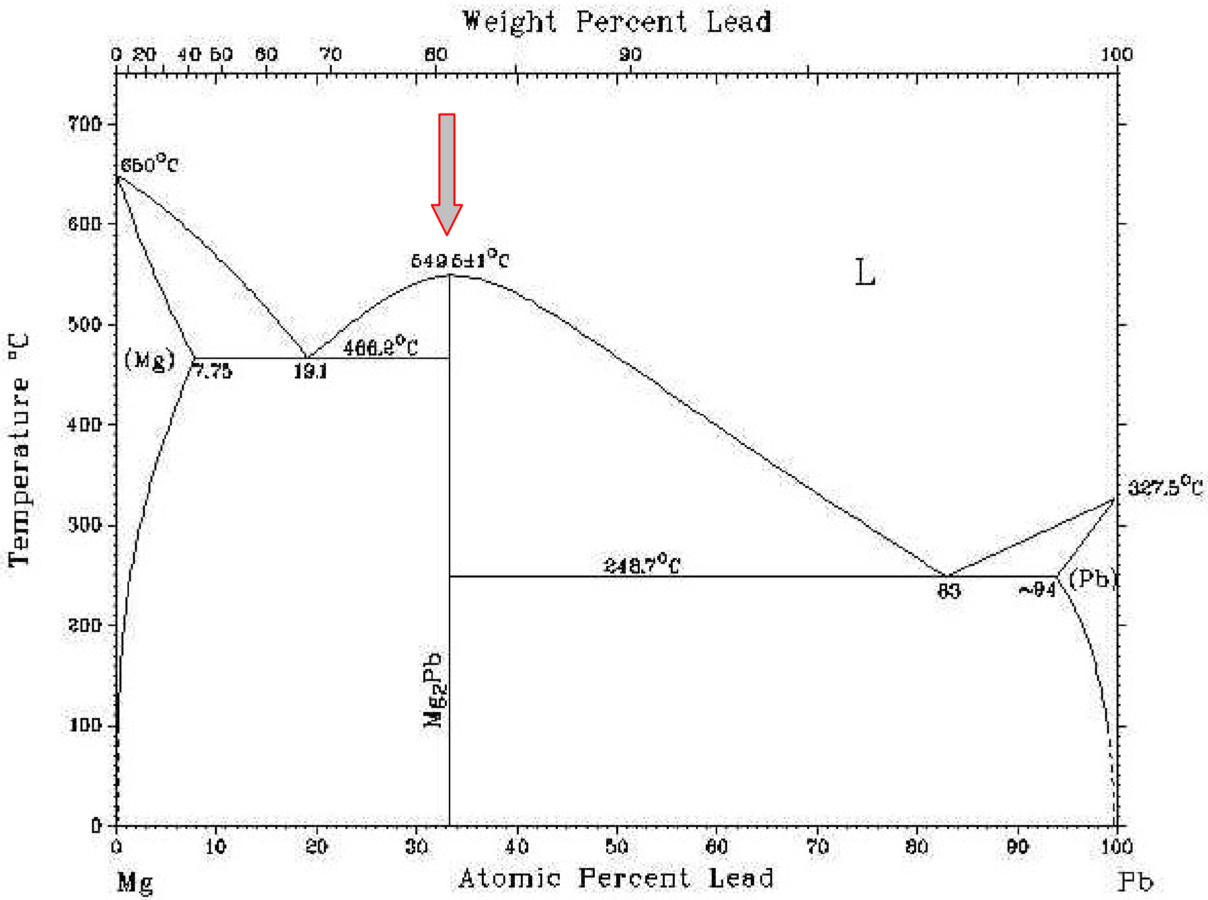

形成稳定化合物

K-Na

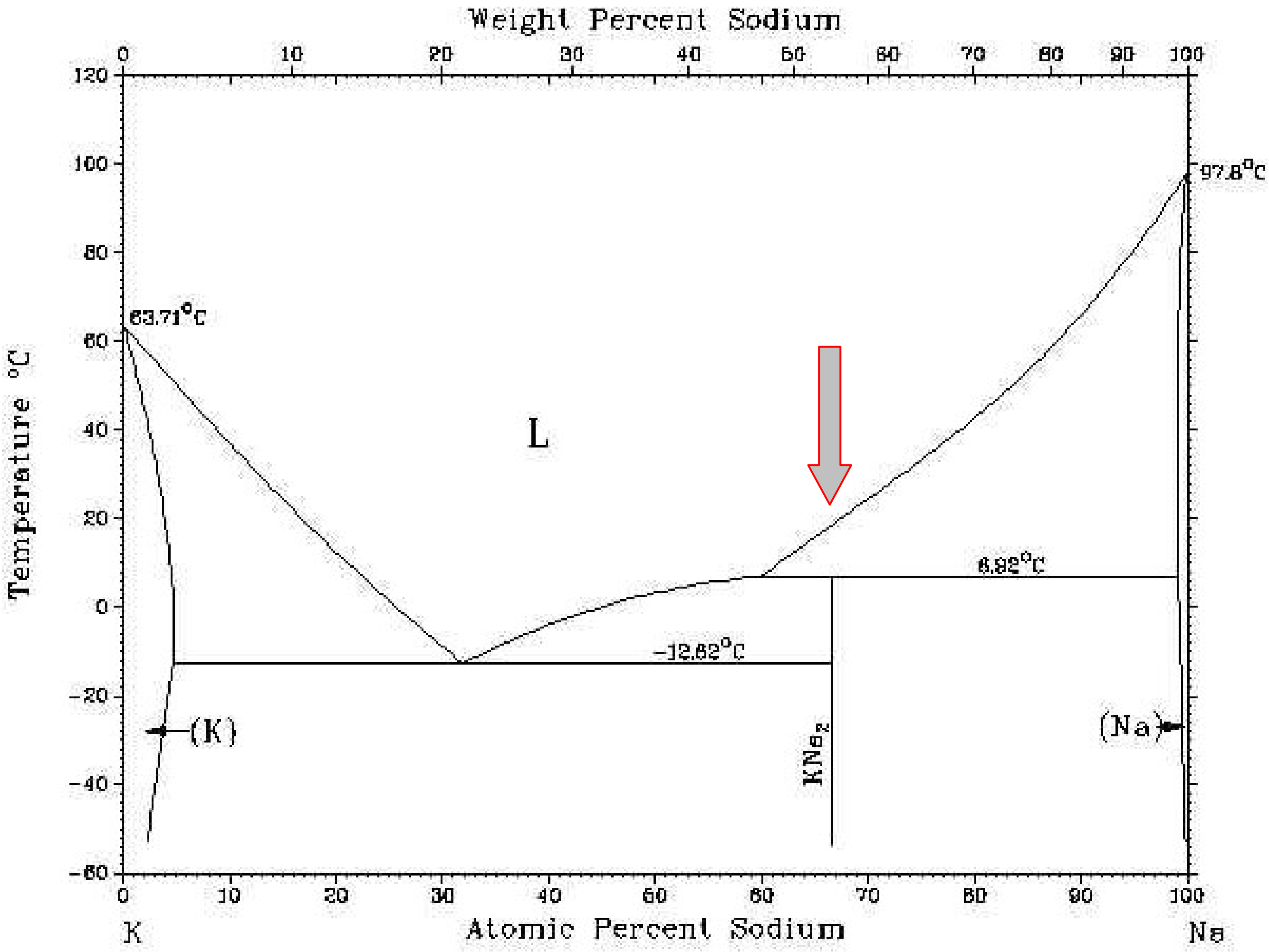

具有不稳定化合物

Ni-Ti

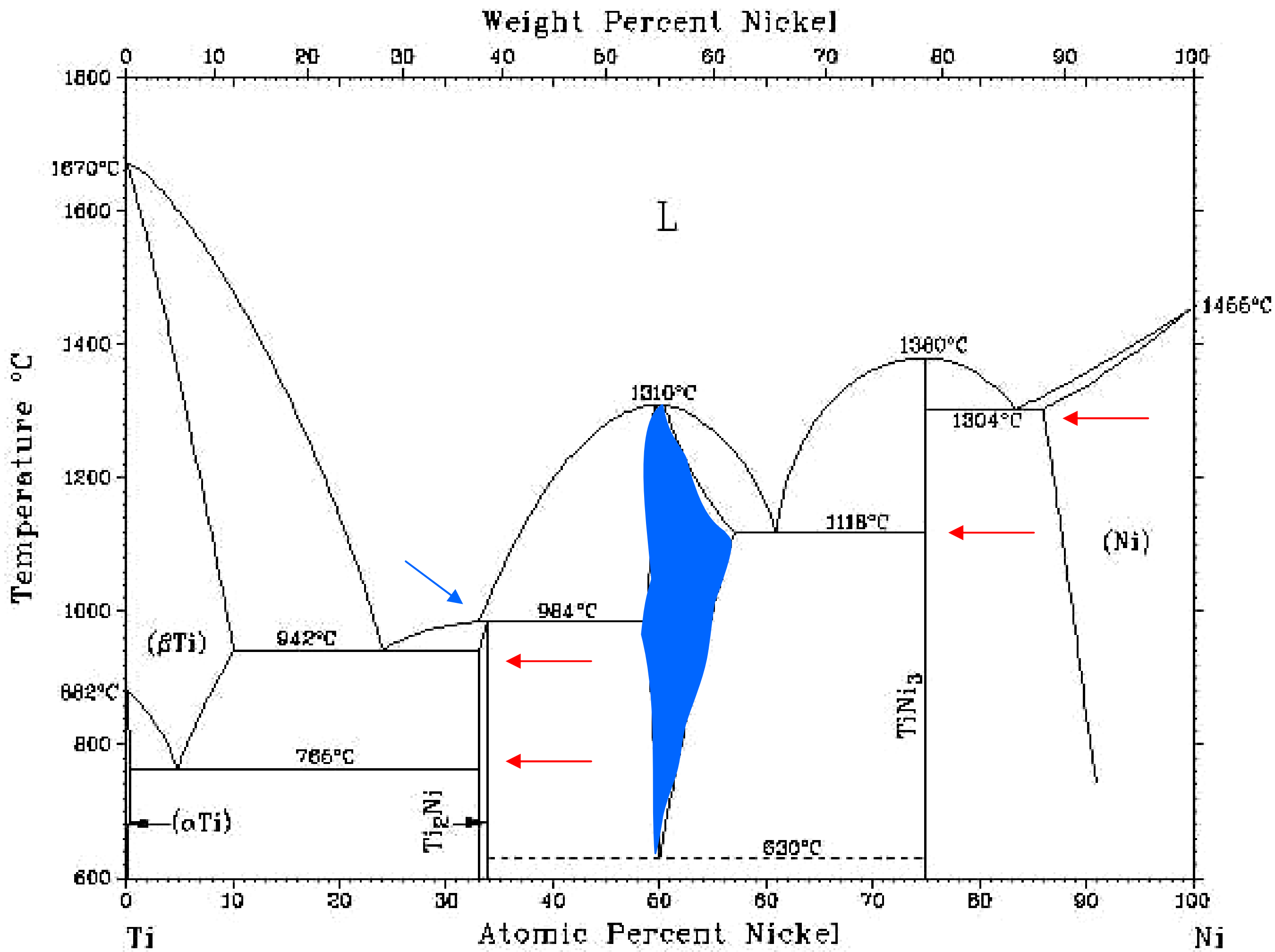
Weight Percent Nickel
0
10
20
30
40
50
60
70
80
90
100
1800
1670°C
1600
1400
1200
1000
882°C
800
600
L
1455°C
1380°C
1310°C
1304°C
1118°C
984°C
942°C
765°C
630°C
(βTi)
(αTi)
(Ni)
Ti_2Ni
$TiNi_3$
Temperature °C
Atomic Percent Nickel
Ti
Ni

Summary of Binary Phase Diagrams

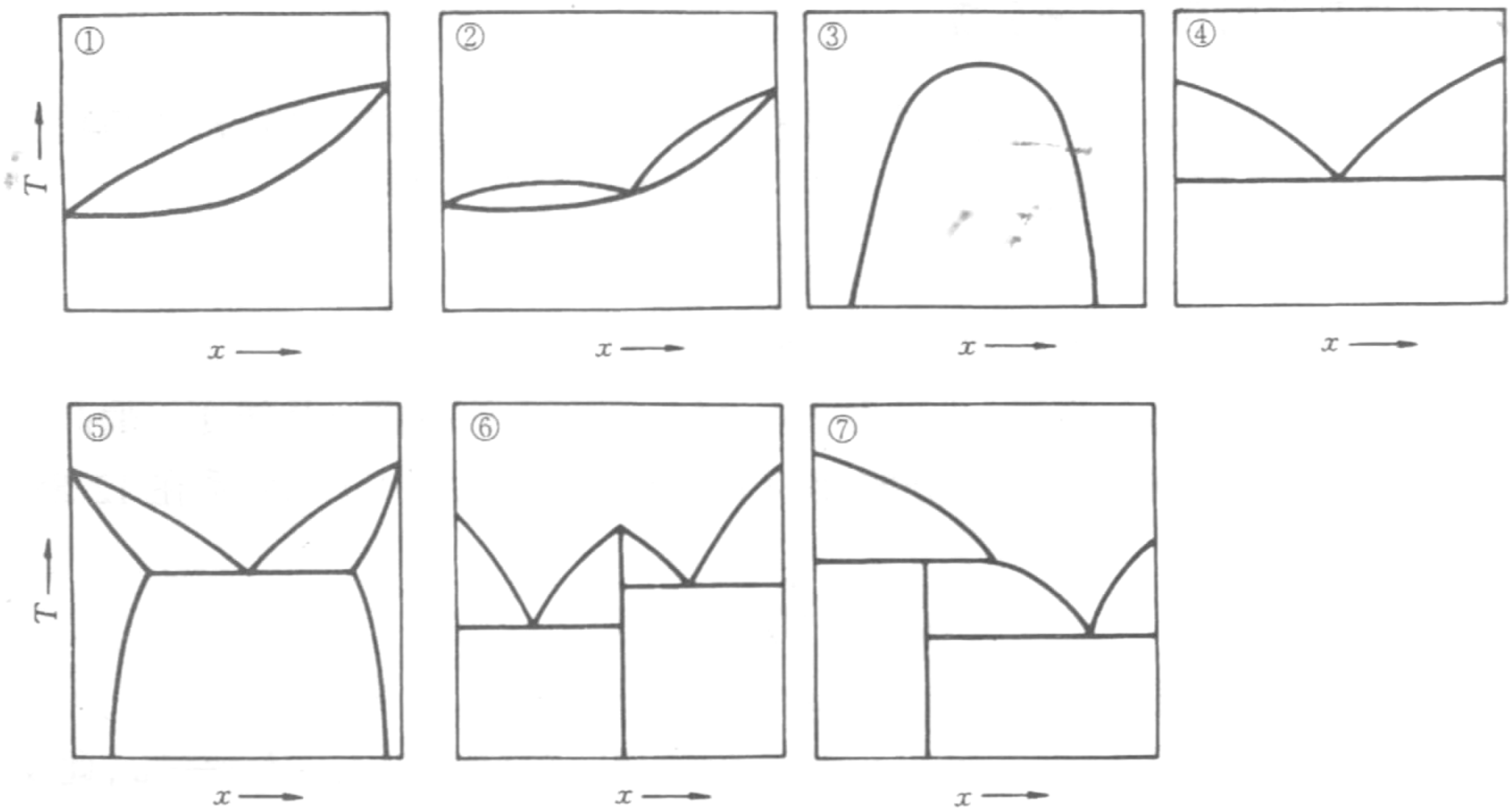

图 6－25　二元相图的 7 种基本类型

Ternary Phases Reaction in Binary Systems

表 6－1　二元系的各种三相平衡反应

转　变　类　型		反　应　式	图　型　特　征
共晶型	共晶转变	$l \rightleftharpoons \alpha + \beta$	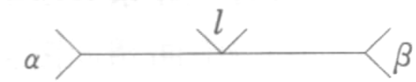
	共析转变	$\gamma \rightleftharpoons \alpha + \beta$	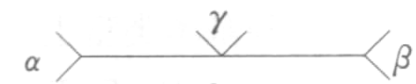
	偏晶转变	$l_1 \rightleftharpoons l_2 + \alpha$	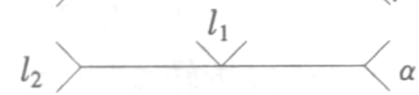
	熔晶转变	$\delta \rightleftharpoons l + \gamma$	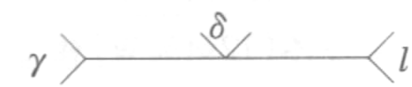
包晶型	包晶转变	$l + \beta \rightleftharpoons \alpha$	
	包析转变	$\gamma + \beta \rightleftharpoons \alpha$	
	合晶转变	$l_1 + l_2 \rightleftharpoons \alpha$	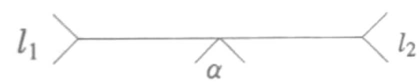

Some phase diagrams for ceramics

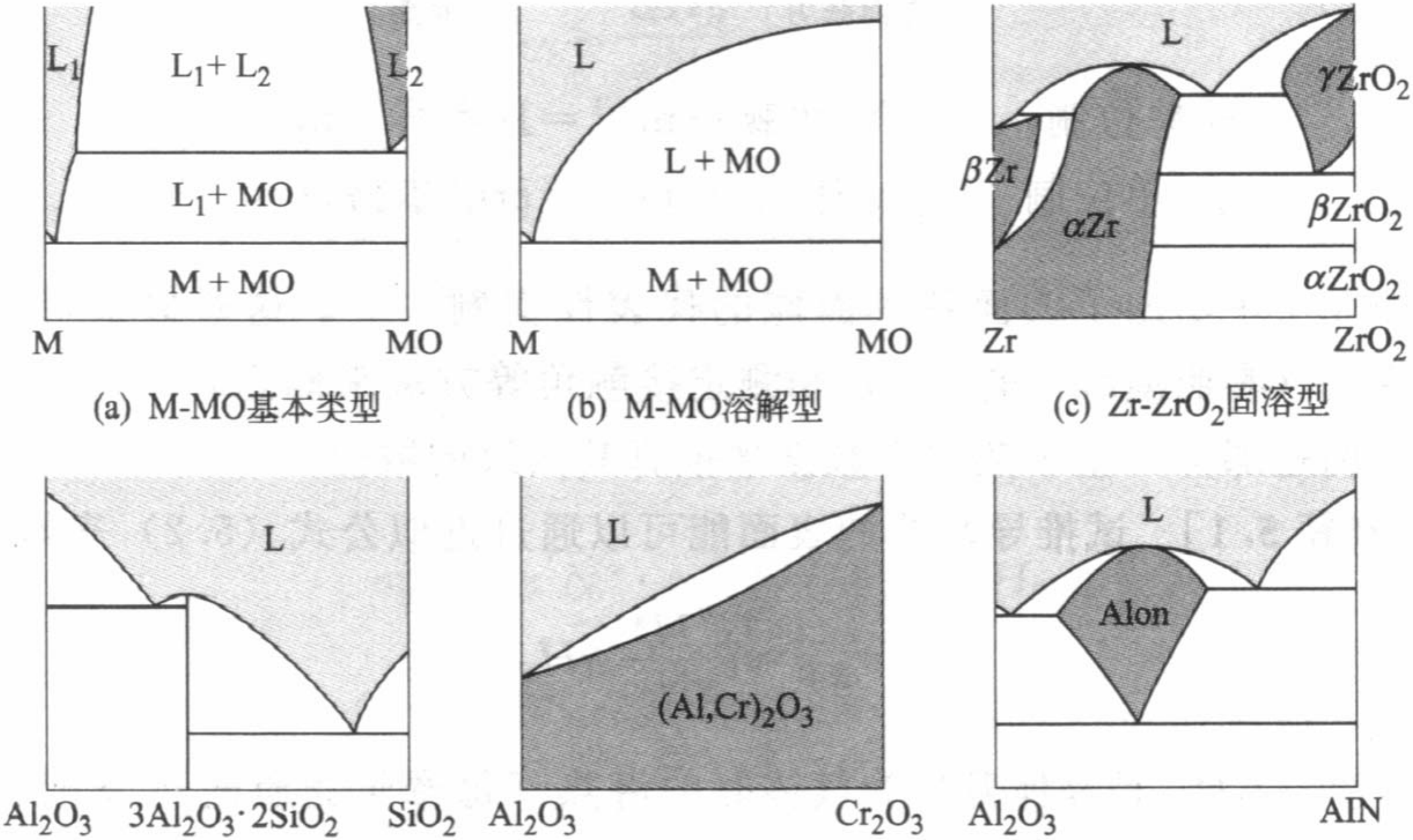

(a) M-MO基本类型　(b) M-MO溶解型　(c) Zr-ZrO_2固溶型

(d) Al_2O_3-SiO_2　(e) Al_2O_3-Cr_2O_3　(f) Al_2O_3-AlN

图 4　典型的陶瓷系相图

（a），（b），（c）为金属-氧化物系；（d），（e），（f）为陶瓷复合系

二元相图构成的规则

- 相图中所有的线条都代表发生相转变的温度和平衡相的成分，相界线是相平衡的体现，平衡成分必沿着相界线随温度变化；
- 两个单相区之间必有一个由这两个相组成的两相区隔开，而不能以一条线接界；两个两相区必须以单相区或三相水平线隔开。相区接触法则：在二元相图中，相邻相区的相数差为1，相数差大于1的相区只能相交于一点；
- 二元相图中，三相平衡必为一水平线，表示恒温反应，三个单相区分别交于水平线上的三个点，其中两点在水平线的两端，另一点在端点之间。
- 与三相线相接的两相区与单相区的相界线的延长线必须进入两相区，而不能进入单相区。

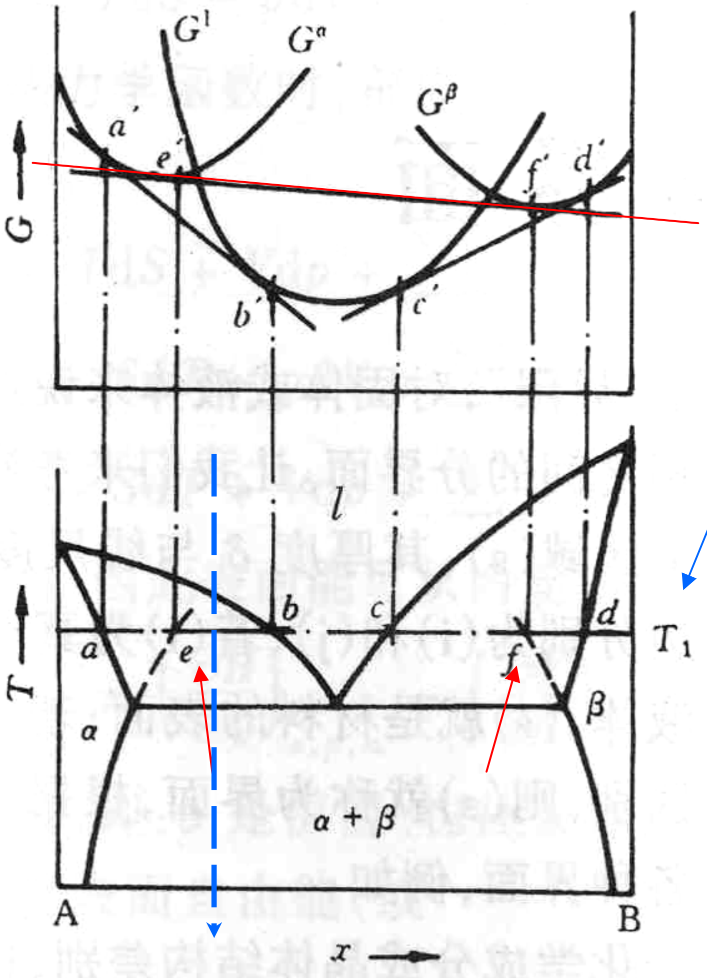

T_1

相图的测定

通过实验测量和观察材料中的某个或某些性质的变化来确定材料中的相平衡关系，并绘制出相图。

动态法/静态法
测定手段
样品的合成方式

相图集

至今，人们已积累了大量珍贵的实测相图数据，大部分被汇编成册并得到广泛应用。

M. Hansen，1936年，二元合金相图

T. B. Massalski，1986年，二元合金相图

印度金属学会，三元铁合金相图集，四元铁合金相图集，三元镍合金相图集

俄巴依科夫研究所，三元合金状态图集

德国金属学会，三元合金相图集

我国昆明贵金属研究所，贵金属合金相图集

美国国家标准研究所，陶瓷学家用相图

相图的用处

- 处理系统是多种物质的复杂系统
  - 相律
  - 相图

    说明系统在不同条件下以哪几相共存；当温度、压力、组成改变时会出现什么相变化各相存在的范围，相变发生的条件等

探索新材料

分析合金组织、化学成分、制定生产和热处理工艺的重要依据！

相图的用处 2

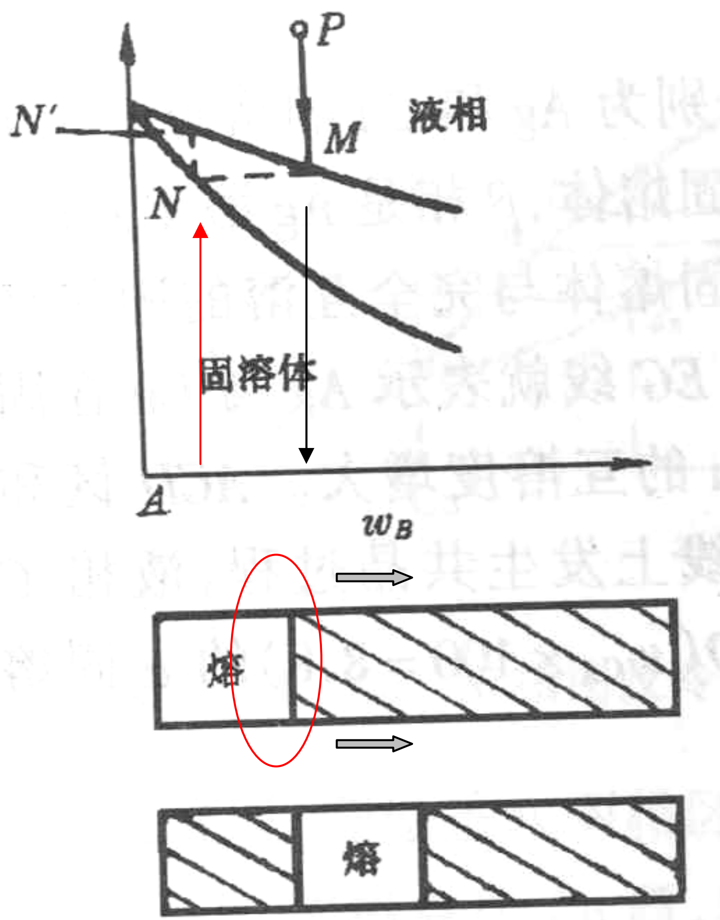

图 5－15　区域熔炼示意图

区域熔炼提纯

析出固溶体杂质的含量比平衡液相的少

相图的用处 3

- 估算热力学数据，如熔化热
  - 从相图上查出一定成分的合金系统中，作为溶剂的金属熔点降低了多少度，然后用稀溶液凝固点下降的依数性公式，即可估算溶剂金属的摩尔熔化焓

$$x_B = \frac{L(T_m - T)}{RT_m^2}$$

相图的用处 4

- 求出活度数据
  - 在两相共存区，某组分在这两个共存相中的化学势应相等

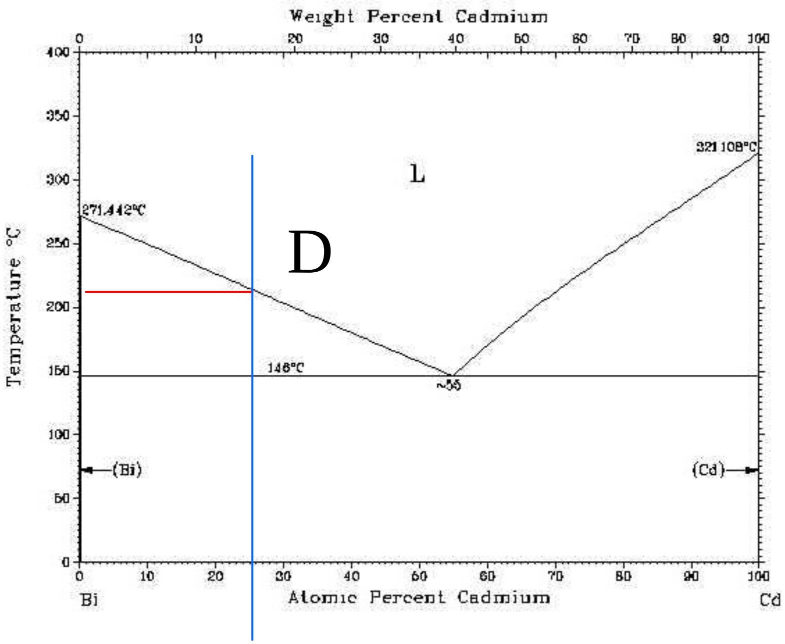

$$\mu_{Bi}(s\ln) = \mu^*_{Bi(s)}$$

$$\mu_{Bi}(s\ln) = \mu^0_{Bi} + RT\ln a_{Bi} = \mu^*_{Bi(l)} + RT\ln a_{Bi}$$

$$\Delta G = \mu^*_{Bi(l)} - \mu^*_{Bi(s)} \quad T \to T_m$$

Solid -> liquid

$$\Delta G = \Delta H_m - T\Delta S_m = \Delta H_m(1 - \frac{T}{T_m})$$

First metallic glass made from rapid solidification

"Duwez's Stupid Alloys"

September 3, 1960 NATURE 869

Non-crystalline Structure in Solidified Gold–Silicon Alloys

Non-crystalline Structure in Solidified Gold–Silicon Alloys

EXCEPT for thin films deposited at very low temperatures[1], highly disordered arrangements of the atoms, similar to that of the liquid state, have never been observed in solid metals and alloys. For some metalloids, the bonding of which may actually be more covalent than metallic, such amorphous configurations have been retained in the solid state[2] by cooling from the melt with sufficient celerity so as to prevent formation of the equilibrium crystalline structures.

It is thus conceivable that such non-crystalline structures can be obtained for some, perhaps all, metals and alloys by quenching rapidly enough from the molten state. In the course of experimentation with the apparatus developed by us[3], an amorphous structure has been detected in a 25 atomic per cent silicon–gold alloy which was quenched from $\sim 1{,}300°$ C. to room temperature.

The quenched alloy was studied by means of X-ray diffraction. A flake (area $\sim 0{\cdot}2$ mm.^{2}; thickness $\sim 10\mu$) was mounted in a Debye–Scherrer camera and exposed to copper K radiation. Intensity (on an approximately linear scale), as obtained from the film with a microphotometer, is plotted against $\sin\theta/\lambda$ in Fig. 1.

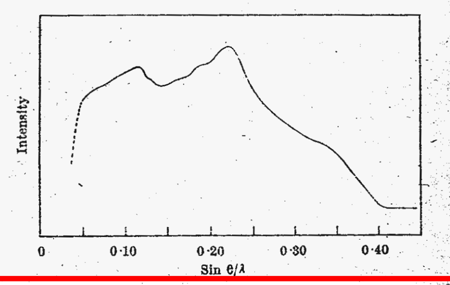

Fig. 1. X-ray diffraction pattern of gold–silicon alloy

It is to be emphasized that the amorphous foil is quite unstable at room temperature (and it is entirely possible that some decomposition could have occurred during the 3-hr. exposure). The decomposition products detected after 24 hr. at room temperature have complex crystal structures, involving d-spacings of the order of 11–12 Å. It is quite probable that many phases may be present under these non-equilibrium conditions. However, at this stage of decomposition, the equilibrium phases are definitely not present.

Since the synthesis and investigation of these amorphous foils are highly uncertain under the present experimental conditions, refinement of the apparatus so as to permit operation at liquid-nitrogen temperatures is now under way. Among the various facets of such non-crystalline metals and alloys which might be of interest, possible superconducting properties should be considered—especially since Buckel[1] has observed that certain metals in thin evaporated layers (amorphous structure) become superconducting at somewhat higher temperatures than with the normal crystal structures.

This work was jointly supported by the Office of Naval Research and the U.S. Atomic Energy Commission.

W. KLEMENT, JUN.
R. H. WILLENS
POL DUWEZ

Division of Engineering,
California Institute of Technology,
Pasadena, California.

W. KLEMENT, JUN.
R. H. WILLENS
POL DUWEZ

[1] Buckel, W., *Z. Physik*, 138, 136 (1954).
[2] Krebs, H., and Schultze-Gebhardt, F., *Acta Cryst.*, 8, 412 (1955).
[3] Pol Duwez, Willen, R. H., and Klement, jun., W., *J. App. Phys.* 31, 1136 (1960).

Non-crystalline

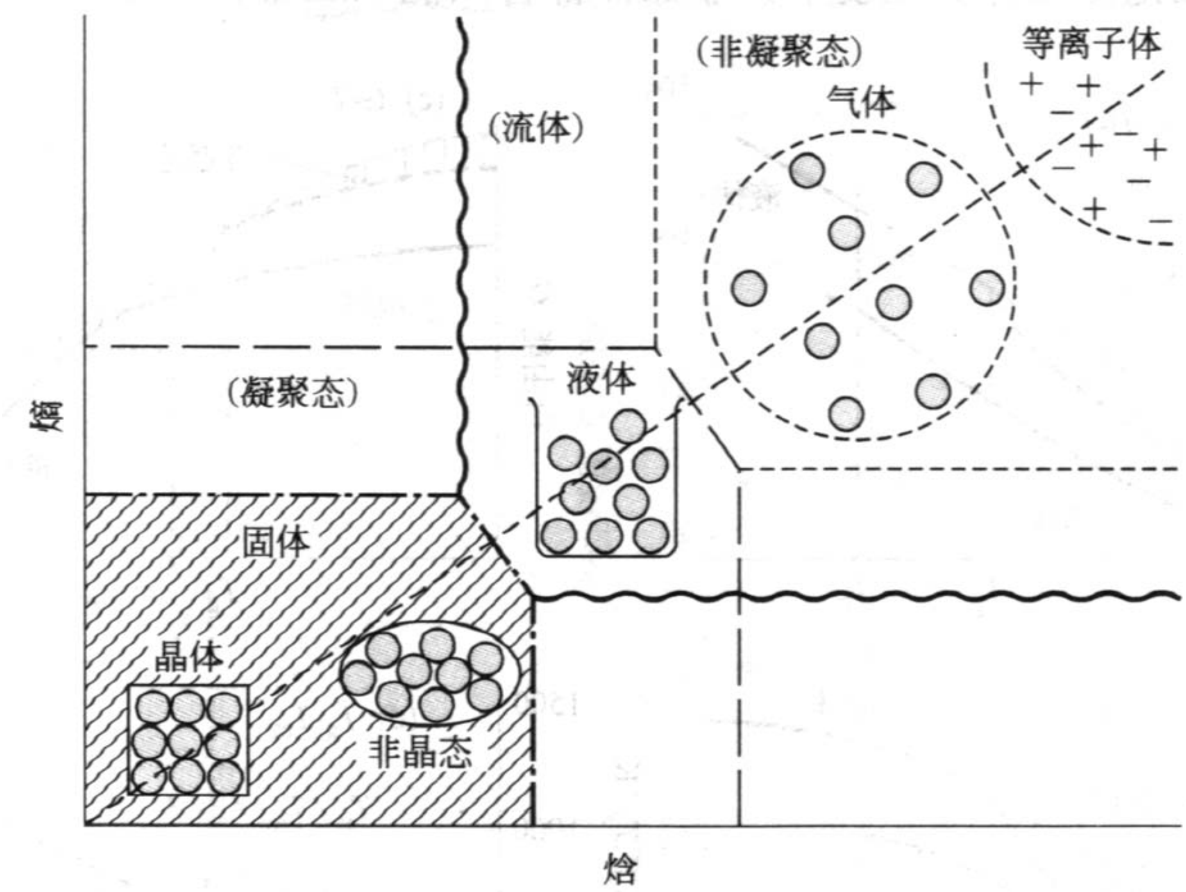

图 2.20　物质的诸状态，非晶态可分类在固体中

From T. Nishizawa

Properties of non-crystalline

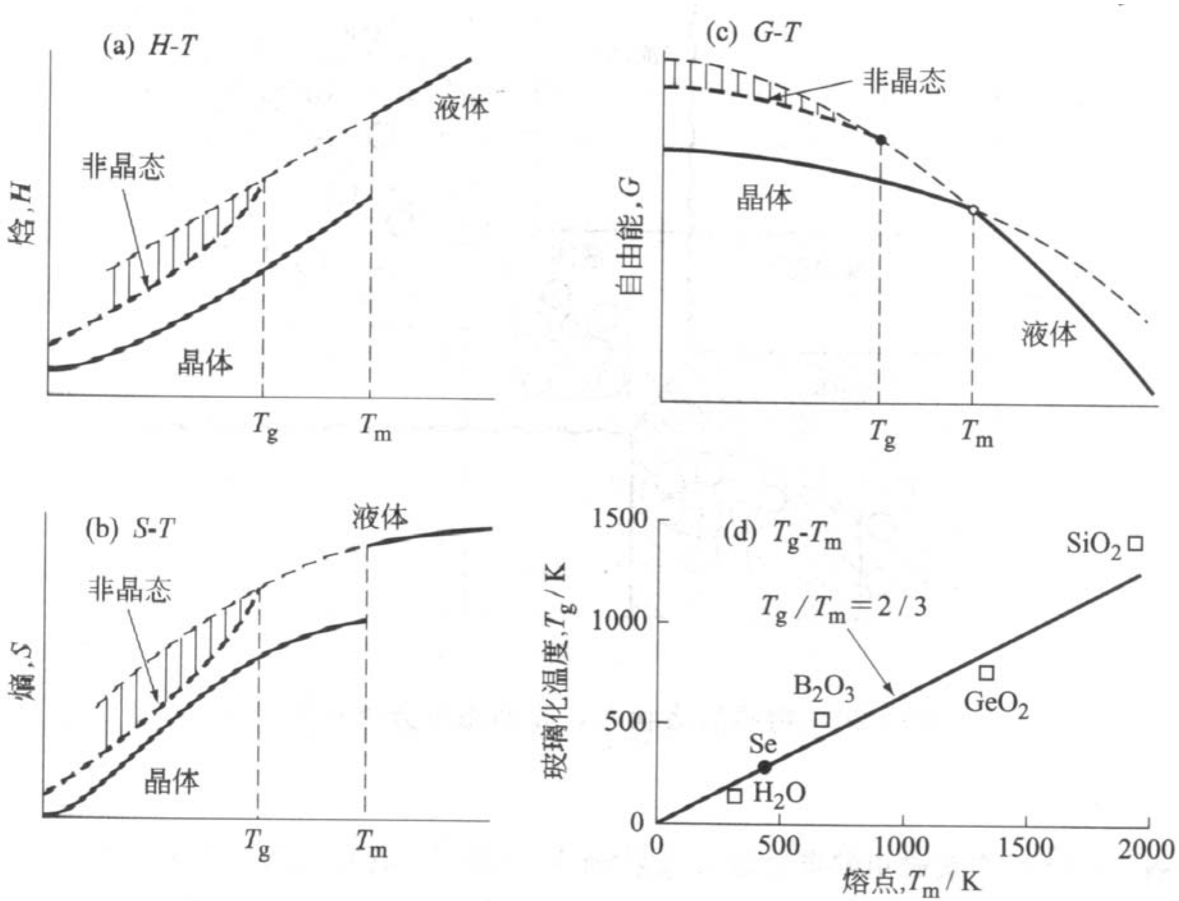

图 2.21 非晶相的焓、熵和自由能的略图及玻璃化温度的测定实例
（非晶相的本质尚不详，未知点尚多）

From T. Nishizawa

非　晶

Au-Si Phase Diagram

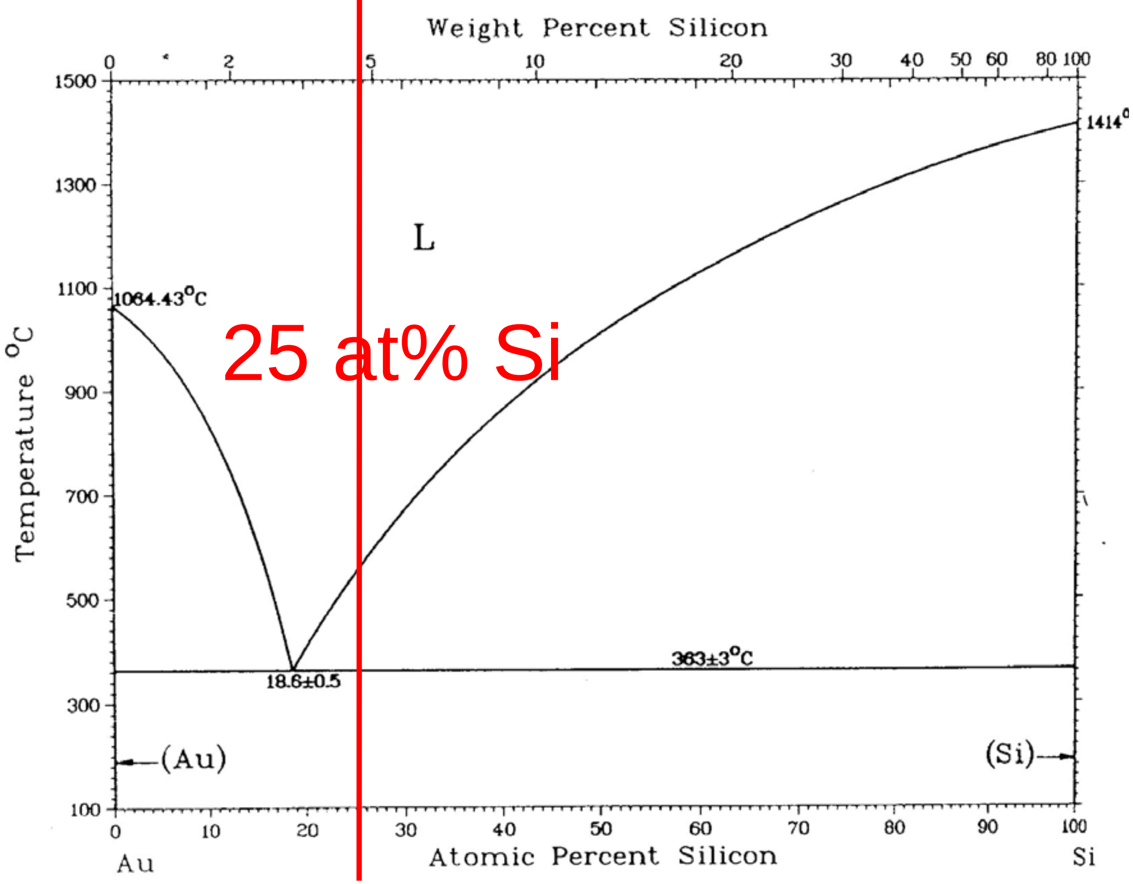

A deep eutectic binary system

Fabrication of Non-crystalline

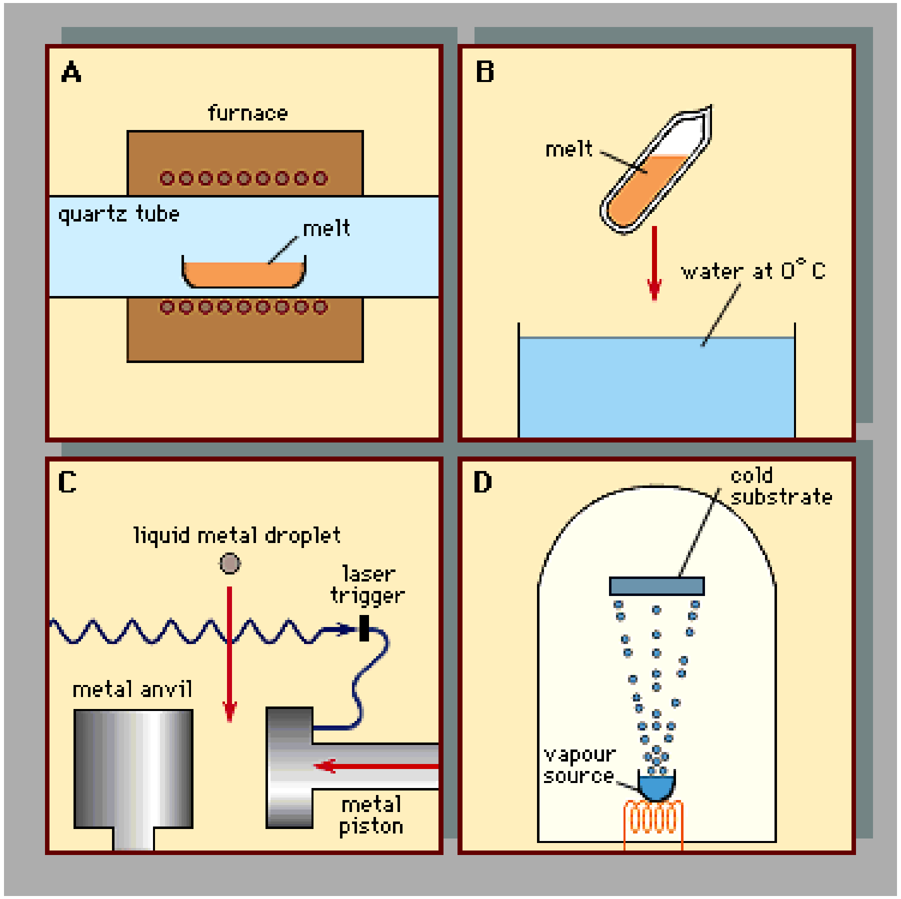

Four methods for preparing amorphous solids. (A) Slow cooling, (B) moderate quenching, (C) rapid splat quenching, and (D) condensation from the gas phase.

From R. Zallen, The Physics of Amorphous Solids, copyright © 1983 John Wiley & Sons, Inc.; reprinted by permission of John Wiley & Sons, Inc.

Applications

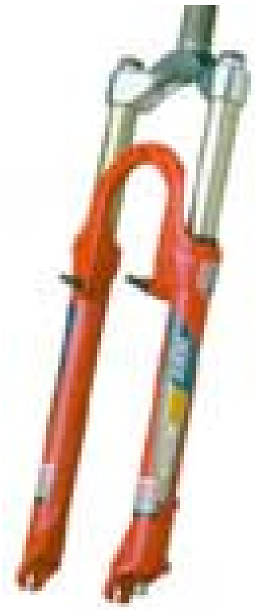

Data from W L Johnson

Ice VI

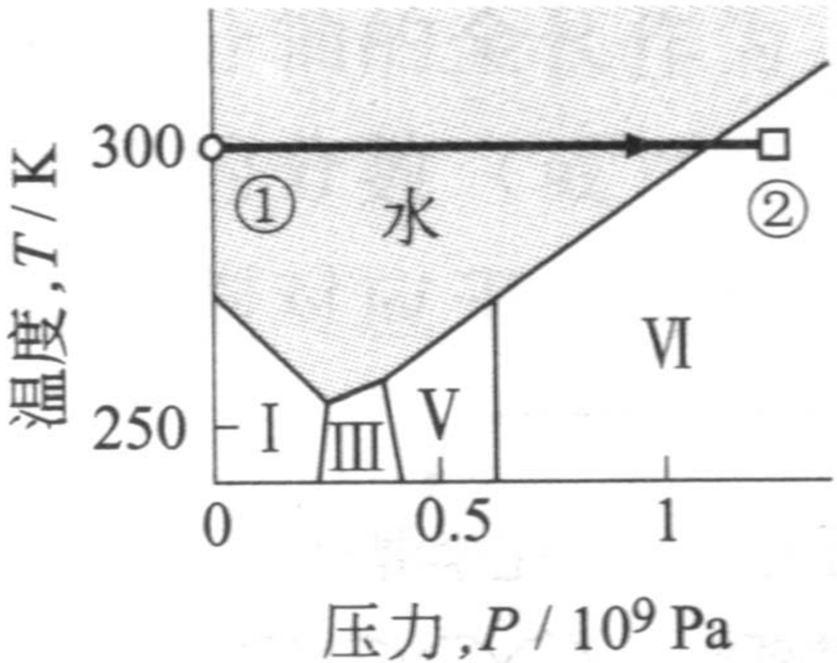

(a) H_2O的P-T图

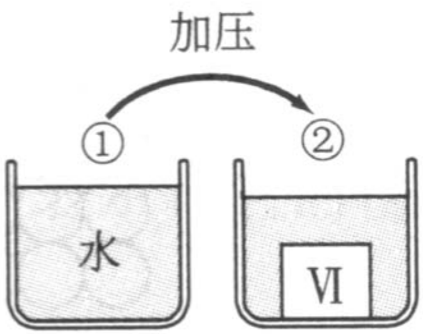

比水重，室温也不熔化的冰

P. W. Bridgman

溶剂法制备金刚石

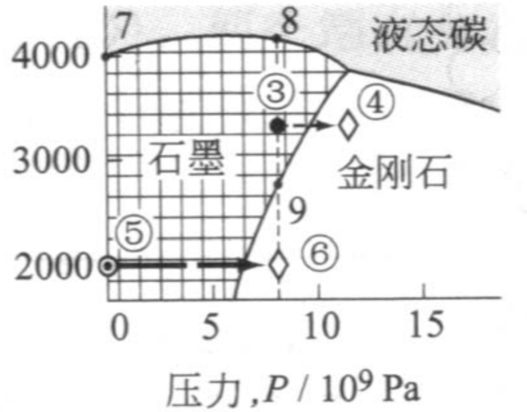

(a) 碳的P-T图

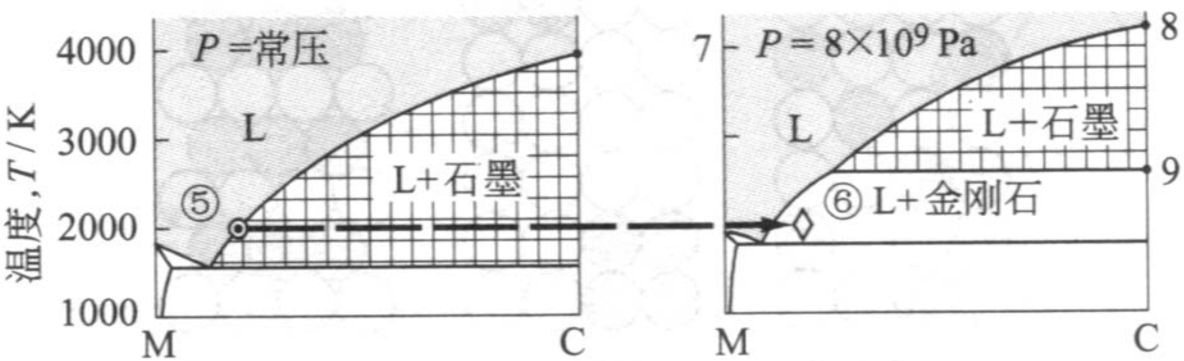

(c) 溶剂(M)-碳系统相图

1010 Pa + 3000 K

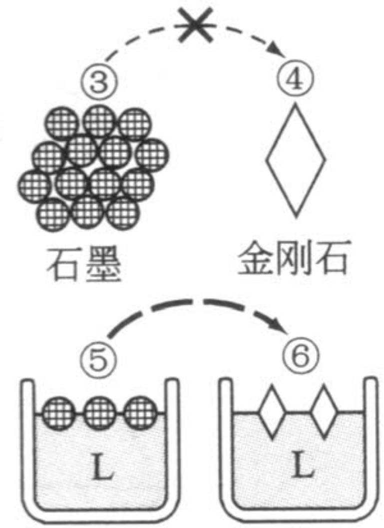

溶剂法

From T. Nishizawa

溶剂法，GE，1955年

将原子活动迅速的液相作为制备的媒体！

二元例题 1

10. 用相律判断下列相图是否正确？说出理由。

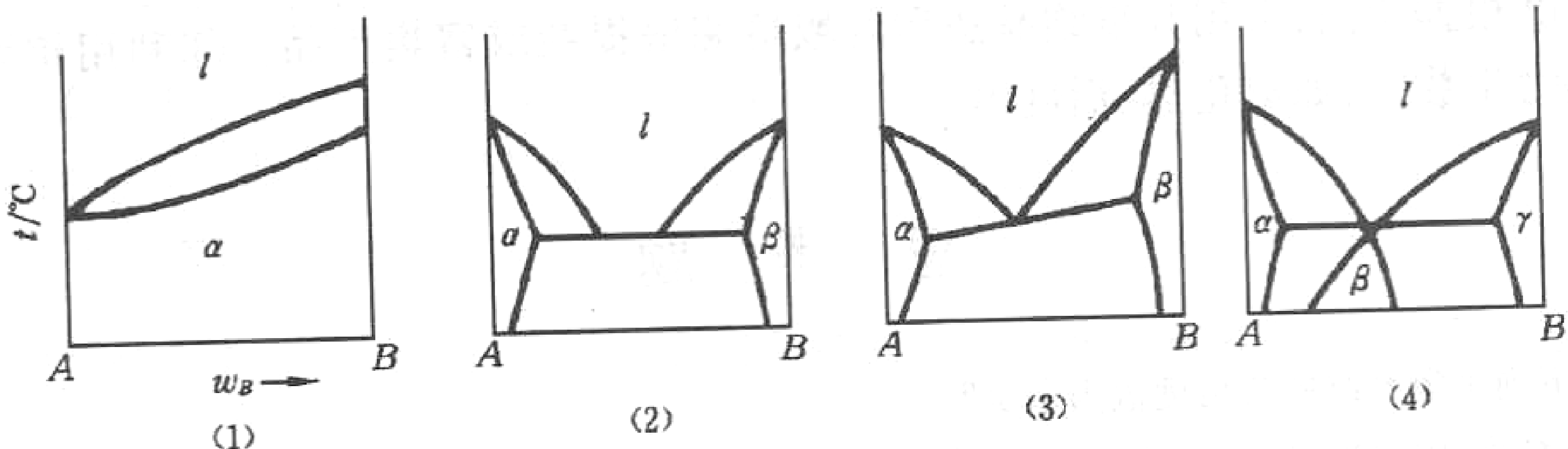

图中 A 及 B 是纯物质，l 指液态，α、β 及 γ 均是固熔体。

二元例题 2

- What is the most stable state of the system at an average composition of X_0?
- Suppose the α-phase was somehow prevented from forming (i.e., consider the equilibrium under the constraint that the α-phase is absent). In this case, what would be the equilibrium state of the system with average composition X_0?

Molar Gibbs free energy of solution, drawn at T and P constant for an α phase and β phase.

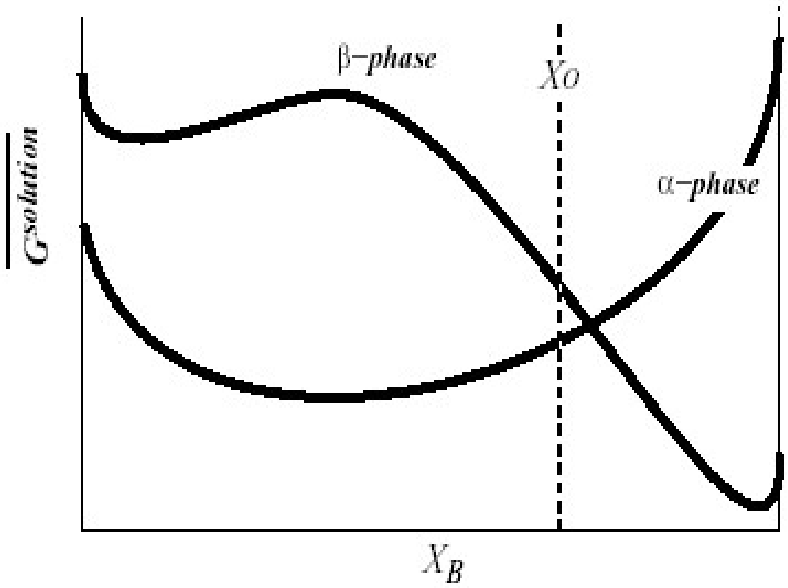

二元例题 3

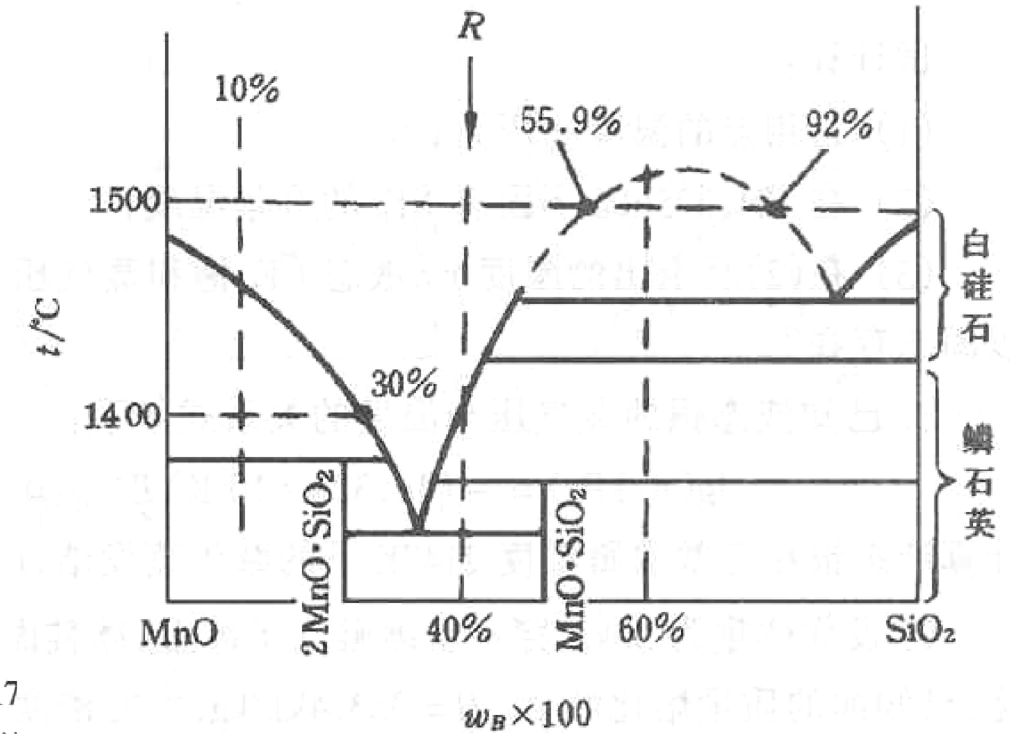

MnO－SiO_2 相图

（1）指出各区域所存在的是什么相？

（2）$w(SiO_2)=0.40$ 的系统（图中 R 点）从 17
1000℃时的冷却曲线示意图。注明每一阶段系纟
发生了哪些变化？指出自由度数为多少？

（3）$w(SiO_2)=0.10$ 的系统 9kg，冷却到 1400℃时，液相中含 MnO 多少 kg？

（4）$w(SiO_2)=0.60$ 的合金 1500℃各以哪些相存在？计算其相对量。

Review of Today

- Spinodal Points
- Compounds
- Summary of Binary Phase
- Ternary Phases Reaction in Binary Systems
- 二元相图构成的规则

Homework

- Exercises in Chap 6

  P 234, 9.6, 9.9, 9.13